Self-folding with shape memory composites at the millimeter scale

S M Felton, K P Becker, D M Aukes, R J Wood

Harvard University, 60 Oxford st, Cambridge, MA 02138 USA

E-mail: `sam@seas.harvard.edu`

December 2014

Abstract. Self-folding is an effective method for creating 3D shapes from flat sheets. In particular, shape memory composites - laminates containing shape memory polymers - have been used to self-fold complex structures and machines. To date, however, these composites have been limited to feature sizes larger than one centimeter. We present a new shape memory composite capable of folding millimeter-scale features. This technique can be activated by a global heat source for simultaneous folding, or by resistive heaters for sequential folding. It is capable of feature sizes ranging from 0.5 to 40 mm, and is compatible with multiple laminate compositions. We demonstrate the ability to produce complex structures and mechanisms by building two self-folding pieces: a model ship and a model bumblebee .

1. Introduction

Self-folding is a fabrication technique in which a flat structure bends itself along hinges, resulting in three-dimensional features [1]. This method has two general categories of applications. The first is in the assembly of structures that are difficult to reach and manipulate. Examples include self-folding within the body [2], in space [3], or at sizes that are too small for manual manipulation [4]. The second application is to speed up and parallelize foldable structures. For example, a manually folded robot can take up to one hour to fold by hand [5]. A similarly sized self-folding robot can fold itself in about five minutes [6].

A variety of self-folding methods have been demonstrated, actuated by many different physical forces including magnetism [7], differential stress [8], polymer swelling [9], pneumatics [10], and shape memory materials [11, 12]. Each has applications for which it is suited. For example, Malachowski et al. used differential stress to activate *in vivo* cell grippers because the sacrificial layer could easily be dissolved in biofluids [2]. Keller used a shape memory alloy to create wires that could tie themselves into knots because each fold could occur in succession [13].

Shape memory composites are self-folding laminates that have been used for creating relatively complex shapes and dynamic machines [6, 14]. Shape memory composites consist of one or more layers of a shape memory polymer (SMP) laminated with one or more structural layers [15, 16]. The SMP is activated by heating, either by light [17], joule heating from embedded resistors [15, 17], or an oven [16, 17], and this induces a contractile stress in the SMP. The stress causes it to pull on the bonded substrate layer. The substrate is mechanically weakened along hinge lines so that when the SMP pulls on either side of the hinge, the substrate can fold along the line. This technique has been used to self-fold structures and machines at length scales from 3 to 20 cm [6, 15]. It is capable of both sequential and simultaneous folding, and the laminate construction means different materials can be integrated into the structure [18]. However, these composites are unable to fold features less than one centimeter in length. On smaller faces, the SMP delaminates from the substrate, preventing folding. We have conducted preliminary research into a new composite that can fold hinges as small as one millimeter [19]. However, the hinges in this composite have to be activated simultaneously due to uniform heating. Additionally, the adhesive used to bond the layers was not adequate, resulting in delamination and imprecise folds.

When selecting a self-folding method for fabrication, there are two major capabilities to consider. The first is whether the method allows for sequential folds. Generally, simultaneously folding all hinges is simpler, but sequential folding allows for more complex geometries, especially if the folded structure is mechanically coupling to another feature, such as a tab locking into a slot, or over a motor shaft [6, 15]. The second capability is the range of length scales that can be folded. The maximum face length generally limits the overall size of the self-folding structure, and is usually proportional to the maximum torque the self-folding hinge can exert. The minimum face size limits the feature resolution, and this limit is often a consequence of fabrication techniques, including machining resolution and adhesion between layers. In addition to strict size limitations, another important measurement is the ratio between maximum and minimum feature size, which correlates with machine complexity. If the maximum length defines structure size and the minimum length defines feature size, the ratio indicates how many features can be built into the structure.

In this paper we present an improved shape memory composite capable of folding faces at length scales ranging from 0.5 to 40 mm. This is accomplished through thinner materials, new machining techniques, new adhesion layers, and additional structural layers to prevent delamination. We demonstrate simultaneous folding of an aluminum-based composite activated by a hot plate, and sequential folding of an FR-4-based composite activated by internal joule heating.

2. Design and Fabrication

The composite consists of three different materials in seven layers (Fig. 1). In the middle is the flexural layer, a 7.5 μm thick polyimide film (440, Chemplex). On either side of the flexural layer is a sublaminate consisting of the contractile SMP, polyolefin (DU-POF-1000-8, U.S. Packaging & Wrapping), sandwiched between two substrate layers.

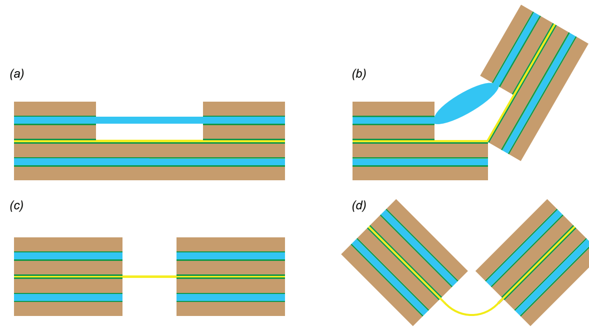

Figure 1. The self-folding composite consists of three functional materials comprising seven layers: The substrate (brown), the polyolefin shape memory polymer (SMP, blue) and the polyimide flexural layer (yellow). These are bonded together with an acrylic adhesive (green). This composite can be programmed with self-folding hinges (a). Folding is induced by activating the SMP, causing it to contract (b). The composite can also be programmed with passive hinges that can bend repeatedly (c, d). This figure is adapted from a previous publication [19].

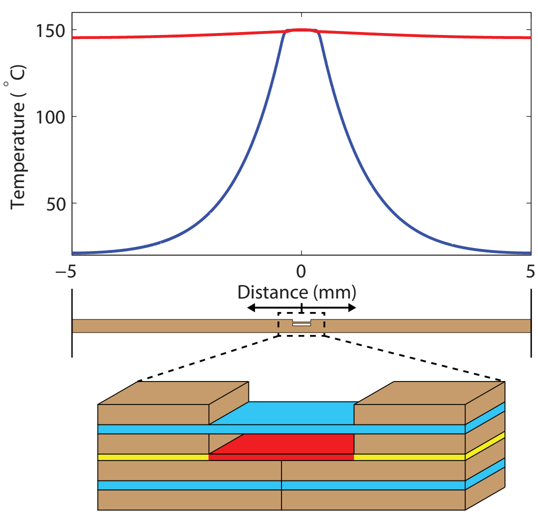

Figure 2. A thermal finite element model of the hinge was built in order to determine the temperature profile of the SMP when the hinge is internally heated to 150° C. The red line indicates the temperature profile of the polyolefin when the substrate is aluminum, and the blue line is the temperature profile when the substrate is FR-4. A diagram of the model hinge is shown below at scale with the graph, and below that a section is blown up to illustrate the hinge geometry. In this figure, red indicates the volume of the hinge which is generating heat.

The layers are bonded together with a 5 μm thick acrylic tape (82600, 3M).

Folding is triggered by heat. When an unconstrained SMP sheet is heated above 130° C, it contracts bidirectionally to 25% of its original length and width. However, when embedded in the composite, the SMP is fixed in place by the substrate except along the self-folding hinges, where the SMP is exposed and allowed to contract. This contraction exerts a shear stress on the composite, causing it to bend. We can activate this process by supplying heat from an external source, such as a hot plate, or we can embed resistive circuits along each hinge. When we supply these circuits with current they release heat and locally activate the SMP.

In order to create a self-folding hinge, layer-specific features were machined into the composite (Fig. 1(a-b)). On the concave side of the fold, a gap was cut into both substrate layers to expose the polyolefin and allow it to contract. The width of this gap varies between 0.2 and 1.8 mm, and is correlated with the final fold angle. On the convex side, a line is cut through the substrate and polyolefin layers so that the flexural layer can bend freely. A passive hinge has similar features (Fig. 1(c-d)). A gap is cut in every layer except the flexural layer. In this case, the gap width affects the hinge stiffness and maximum bend angle.

The substrate can be any sufficiently stiff material. In our devices we use two different substrates: aluminum (1145-H19) in the uniformly heated structures and FR-4 (FR408HR, Isola Group) in the resistively heated structures; in both cases the substrate is 50 μm thick. Aluminum was chosen for the uniformly heated structures because of its high stiffness and high thermal conductivity. This enabled the entire structure to maintain a uniform temperature even when parts of it lost contact with the hot plate, ensuring that folding continued over the entire structure. In contrast, FR-4 was used in the resistively heated structures because of its low thermal conductivity. Some amount of insulation is necessary between adjacent folds to prevent the heat from one hinge to prematurely activate another. In order to compare the thermal dynamics between substrate materials, we developed a thermal finite element model of two composites, one made with aluminum and one with FR-4. The simulation assumed each hinge was generating heat at a constant rate, and the polyolefin temperature at the center was approximately 150° C after 20 seconds. The temperature profile of the SMP layer orthogonal to the hinge in both situations is shown in Figure 2. In the aluminum substrate, the temperature five millimeters from the hinge only dropped to 145° C, while in the FR-4 substrate the same location is 21° C. The transition of an SMP often occurs over a 30° C range, so a difference of at least a 30° C between hinges would be necessary in order to achieve sequential folds.

If the structure requires an embedded circuit, either for resistive heating or for its final function, a copper trace is included onto the flexural layer. Copper is used in the devices presented here because of it is flexible, easy to sputter coat, and has adequate resistivity for our trace geometry. The copper layer is approximately 200 nm thick; however, we found that our sputtering rate varies between 90 and 200 nm/min, so the trace thickness varied commensurately. In most hinges (and unless otherwise noted) the resistive portion of the trace is 800 μm wide and runs coincident to the midline of the hinge.

The composites are assembled in steps alternating between laser machining with a diode pump solid-state laser (DC150H-355, Photonics Industries) and bonding (Fig. 3). First, four substrate layers (T1, T2, B1, B2) are prepared by applying the tape to both

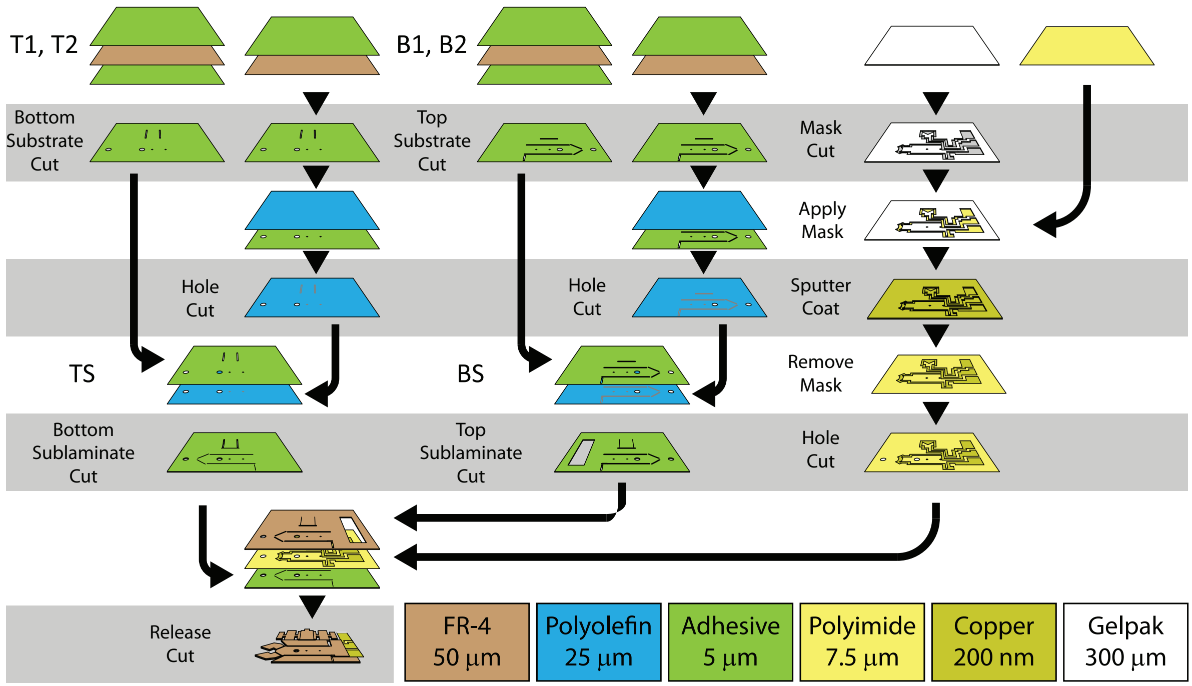

Figure 3. Fabrication occurs in sequential steps alternating between laser machining and bonding layers together.

sides of two layers (T1, B1), and one side of the other two (T2, B2). The tape backing is left on the outer sides of the tape. The features exclusive to the substrate are then machined into the layers. This step uses two different cut patterns: one cut pattern for the substrate layers of the top sublaminate (T1, T2), and one for the layers of the bottom sublaminate (B1, B2). After machining, the polyolefin layers are bonded to T2 and B2 and machined again to remove the polyolefin at the alignment holes. Layers T1 and B1 are then pin-aligned and bonded to the other side of the polyolefin, resulting in two sublaminates (TS and BS). Each is machined with another cut pattern, removing material from both the substrate and polyolefin layers. At this point there is adhesive on one side of the TS and BS sublaminates.

Making the flexural circuit layer requires four steps. First, the flexural thin film is rolled onto a piece of Gel-Pak (WF Film, Delphon Industries), which keeps it flat during handling. A mask made of Gel-Pak is cut with the circuit trace pattern and applied with pressure to the flexural layer. It is then sputter-coated with copper for a total of 110 seconds, after which the mask is removed and alignment holes are machined in both the flexural layer and supporting Gel-Pak. If the flexural layer does not include a circuit, the thin film is still attached to the supporting Gel-Pak and machined, but is not masked or sputter-coated.

Once the flexural layer is prepared and the two sublaminates are machined, the TS sublaminate is pin-aligned and bonded to the exposed side of the flexural layer. The supporting Gel-Pak is then removed, and the BS sublaminate is aligned and bonded to the other side. The complete composite is then machined with the release cut pattern, resulting in the final planar structure. This structure is pressed with approximately 2.5 MPa for 45 minutes. For our resistively heated samples, the composite is secured to a glass slide with double-sided tape and the exposed traces are connected to copper pads with conductive epoxy (8331-14G, MG Chemicals).

3. Model and Results

3.1. Maximum Feature Size

We used a previously published model to predict the maximum face size a self-folding hinge could lift against gravity [19]. The torque per meter of hinge length τ exerted by the hinge is a function of the contractile stress σ of the SMP, the thickness t of the SMP, and the distance d of the SMP from the bending point. The moment due to gravity per meter hinge length M is a function of the areal density ρ and length L of the folding face. For a rectangular face

$$\tau = t\sigma d \tag{1}$$

$$M = g\rho d^2/2 \tag{2}$$

$$\tau = M_{max} \tag{3}$$

$$L_{max} = \sqrt{2t\sigma d/\rho} \tag{4}$$

One difference from previous models of shape memory composites is that this paper refers to the contractile stress of the SMP. Previous papers referenced the Young's modulus of the material and shrink ratio to calculate the contractile stress. However, the mechanical behavior of shape memory polymers can be nonlinear, so it is more accurate to measure the contractile stress directly during transition. This stress was measured by placing a 40 mm wide piece of polyolefin in an Instron material characterization machine and heating it with a heat gun. The material was fixed at a 10 mm length so that the contractile length was significantly shorter than the orthogonal length, similar to the SMP geometry in the hinge. The maximum stress measured was used as the contractile stress in our model. We found that this stress is 2.5 ± 0.3 MPa (range indicates standard deviation, N=8). Other measured values and the expected maximum face lengths for each composite are given in table 1.

We built aluminum test hinges that were 30 mm wide and of varying lengths (30 mm, 40 mm, 50 mm, and 60 mm) to confirm our predictions. These hinges were activated on a hot plate set to 110°C. The 30 and 40 mm long faces folded to completion in approximately 15 s, judged by observing a fold of more than 90°, at which point gravity no longer limits the fold angle. The 50 mm and 60 mm long faces took approximately two minutes to stop moving, and neither folded to completion. The 50 mm face stopped at approximately 46°, and the 60 mm face stopped at approximately 32°. We believe that this is due to the viscoelasticity of the polyolefin in its rubbery state, and that the SMP sheet partially relaxed under the increased load from the faces.

Value	Symbol	Value	Units
Contractile stress	σ	2.5	MPa
SMP thickness	t_p	25	μm
Lever arm	d	66	μm
Torque per meter	τ	4.8	mN-m/m
Density of aluminum composite	ρ_a	616	g/m^2
Density of FR-4 composite	ρ_f	446	g/m^2
Max face length - aluminum	L_{max}	39.7	mm
Max face length - FR-4	L_{max}	46.7	mm

Table 1. Measured and calculated values for determining maximum face size.

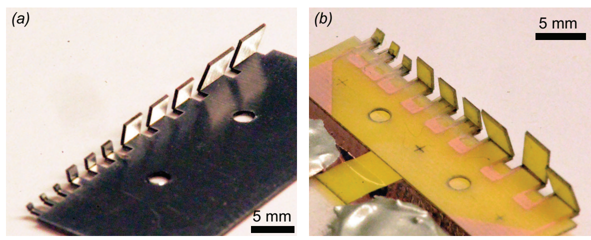

Figure 4. Experimental pieces were built with square faces of variable length to determine the minimum feature size that could be self-folded. (a) A composite with an aluminum substrate was activated by uniform heating from a hot plate, and folded faces from 0.5 to 3 mm in length. (b) A composite with an FR-4 substrate was activated through resistive heating, and successfully folded faces one to three millimeters in length.

3.2. Minimum Feature Size

In order to determine a minimum feature size, we built experimental hinges with square faces of variable lengths. We first built uniformly heated hinges with an aluminum substrate and faces varying from 0.5 to 3 mm long on a single sample (Fig. 4(a)). Each hinge had a 400 μm gap width. The completed sample was placed on a hot plate set to 110° C and left to fold for approximately one minute. These faces all folded successfully. However, there was a noticeable difference in angles, as larger faces folded to sharper angles. We then built resistor-heated hinged with FR-4 and faces from one to three millimeters long (Fig. 4(b)). Smaller faces were not possible because the feature size of the trace and separating gaps were too fine for our masking process. Because of the small size, the resistive traces were 400 μm wide. These faces also folded successfully when supplied with 100 mA of current. However, they showed greater individual variation in final fold angle. This is likely due to the differences in heat profiles at each hinge; different sized hinges have different edge effects where the traces enter and leave the hinge line. In this case, the smaller faces folded at a lower current than the larger faces. When the current was increased to activate the larger faces, the increased heat led to delamination in the smaller faces.

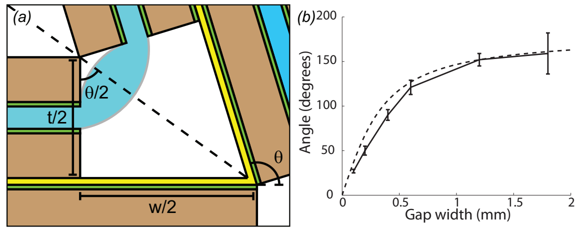

Figure 5. (a) A model for predicting final fold angle based on hinge geometry was developed based on the assumption that folding stopped when the two faces came into contact. The fold angle θ is dependent on the composite thickness t and the width of the gap w cut into the substrate. (b) θ was measured as a function of w (solid line, n=8, error bars indicate standard deviation). These results were compared to an analytical model (dashed line) shown in equation 5.

3.3. Angular Control

We used another previously published analytical model to predict final fold angle based on the gap width [19]. This model assumes that the folding stops when the corners of the substrate on either side of the hinge come into contact, producing a quadrilateral (Fig. 5(a)). Therefore, the fold angle θ is a function of the ratio of the gap width w and composite thickness t and is defined by the equation

$$\theta = 2arctan\,(w/t) \tag{5}$$

We then built experimental hinges consisting of square faces five millimeters long, attached to a stationary base face. These hinges had gap widths of 0.1, 0.2, 0.4, 0.6, 1.2, and 1.8 mm wide. They were supplied with 180 to 250 mA of current for 20 to 60 seconds, until folding was completed. This variation is due to the variable resistivity of the heating trace.

The measured fold angles can be seen in Figure 5(b) as a function of gap width, along with the analytical model. The model overestimates the final fold angle; we believe this may be due to the substrate increasing in thickness as the SMP contracts and thickens. The model predicts that a higher thickness results in a smaller fold angle.

We created more experimental hinges with the same geometries and 0.4 mm gap widths. One of these pieces was made with aluminum, and the other was made with an FR-4 substrate, but without the copper traces. Both were uniformly heated on a hot plate set to 110° C for approximately 15 seconds. The uniformly heated FR-4 hinges folded to a final angle of 82° with a standard deviation of 1°. This demonstrated more precision than the resistively heated hinges with the same gap width, which had a mean final angle of 90° with a standard deviation of 6°. The aluminum hinges folded to a mean final angle of 122° with a standard deviation of 5°. This increase in angle may be due to the increased rigidity of the aluminum, which would better constrain the polyolefin. Constraining the polyolefin would prevent it from thickening, which in turn would keep the composite thickness from increasing. The standard deviation of the aluminum hinges was less than the standard deviation of the resistively heated hinges

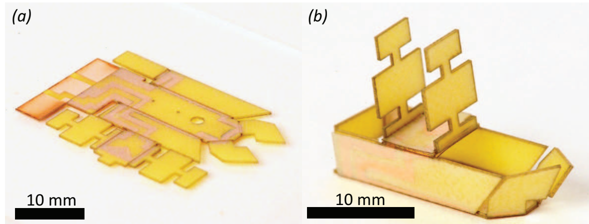

Figure 6. (a) The flat composite programmed to fold into a ship-like structure. (b) The ship after folding.

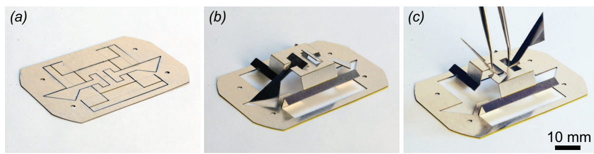

Figure 7. (a) The flat composite programmed to fold into a bumblebee-like structure. (b) The bumblebee after folding. (c) the bumblebee with its wings raised.

with a similar mean fold angle; the resistive hinges with a 0.6mm gap folded to an angle of 121° ± 8°.

3.4. Demonstration Structure: Ship

We designed a structure resembling a miniature ship to demonstrate the complexity of a structure folded sequentially via resistive heating (Fig. 6). This structure assembled through two sequential folding steps (supplemental video). The first folds created the hull of the ship and were activated with 200 mA of current. The second set raised the sails and was activated with 160 mA. Each step took approximately 20 seconds. We believe the difference in activating currents is related to the differences in torque required for the features in each set of folds, as well as differing thermal profiles. The hinges ranged in length from 3 to 13 mm in length, and included both mountain and valley folds.

3.5. Demonstration Structure: Bumblebee

We designed and built a structure that resembled a bumblebee to demonstrate that uniform folding could produce static structures and dynamic mechanisms (Fig. 7). The bumblebee assembled during a single folding step (supplemental video) that was activated by a hot plate set to 110°C. Assembly took eight seconds. This structure includes a self-folding Sarrus linkage which comprises the 'body' of the bee, and wings that are attached to the body via passive hinges. The wings can be actuated by pushing on tabs in the body of the bee. The Sarrus linkage is a single degree-of-freedom mechanism which allows two surfaces to move towards or away from each other while constraining them to remain parallel. This linkage is particularly significant because it forms the basis around which Pop-Up Book MEMS [20, 21] devices are designed, indicating that the self-folding technique presented here is compatible with Pop-Up Book MEMS and could be used to actuate the assembly process. The self-folding hinges ranged in length from 8 to 15 mm in length, and included both mountain and valley folds. The passive hinges were each three millimeters long.

4. Discussion

The self-folding techniques presented here demonstrate a way to automate the assembly of structures and machines. This self-folding technique is appropriate for features from 0.5 to 40 mm long, is compatible with different materials and activation methods, and is more precise than previously demonstrated methods. The minimum feature size is close to the practical limit for folded features because the composite is 0.3 mm thick; If necessary, smaller features can be surface micromachined into the composite. The folding nature of this method means that it is compatible with computational tools such as Origamizer [22] and popupCAD [23], as well as similar mesoscale manufacturing techniques such as Pop-Up Book MEMS [20, 21]. This is also a relatively inexpensive and fast process; For uniformly activated hinges, the only significant piece of equipment needed is a laser cutter with an appropriate resolution. For mass production, the cutting step could be replaced with stamping. Resistively activated hinges also require a means to pattern the trace, but this was performed without a cleanroom or any hazardous materials.

There are still issues with repeatability in this self-folding method. Resistively folded hinges have variable temperature profiles based on the trace geometry, hinge size, and sputtering process, resulting in different temperatures at different hinges. When this issue is combined with the heat sensitivity of the composite, it can result in delamination and inaccurate fold angles. For instance, the polyolefin used in these experiments has a nominal transition temperature of 130°C, yet the adhesive has a nominal maximum operating temperature of 150°C, resulting in a narrow operational range for the composite. If the current is too low, some faces might not fold completely, and if it is too high, other faces might delaminate. When faces delaminate, the joint stops programmed into the composite via gap width are no longer reliable. This issue could be corrected by selecting new materials with different thermal properties, or by adjusting individual features of each hinge, such as the supplied current or the trace width. These adjustments would benefit from a thorough characterization of the SMP, the thermal dynamics, and the hinge behavior. The uniformly heated hinges were more precise, but there was still angular variation depending on the hinge length, which also warrants further investigation.

There is significant and interesting work that can be done to develop design rules for self-folding machines and automate some of this process. We used popupCAD to design the bumblebee; this has demonstrated the potential of folding-focused computer design tools to speed up our prototyping process. Further work could automate the generation of sequential folding steps, trace patterns, and the control system to supply the necessary currents. We are also interested in integrating electromechanical components such as actuators and sensors into our self-folded mechanisms to produce autonomously folding machines. Finally, while we have studied the geometric capabilities of this technique, further work must be done to determine its mechanical properties. For example, the self-folding hinges, while nominally static after cooling, are actually noticeably compliant.

Because of the simplicity of fabrication and flexibility with regards to materials and geometry, we believe that this and other shape memory composites are a valuable method for creating self-folding structures and machines. We expect future research to expand the capabilities and applications of these composites.

Acknowledgments

The authors gratefully acknowledge support from the National Science Foundation (award numbers CCF-1138967 and EFRI-1240383) and the DoD, Air Force Office of Scientific Research, National Defense Science and Engineering Graduate (NDSEG) Fellowship, 32 CFR 168a. Any opinions, findings, and conclusions or recommendations expressed in this material are those of the authors and do not necessarily reflect those of the funding organizations.

References

[1] Leong T G, Zarafshar A M and Gracias D H 2010 *Small* **6** 792–806
[2] Malachowski K, Jamal M, Jin Q, Polat B, Morris C J and Gracias D H 2014 *Nano letters* **14** 4164–4170
[3] Zirbel S A, Lang R J, Thomson M W, Sigel D A, Walkemeyer P E, Trease B P, Magleby S P and Howell L L 2013 *Journal of Mechanical Design* **135** 111005
[4] Na J H, Evans A A, Bae J, Chiappelli M C, Santangelo C D, Lang R J, Hull T C and Hayward R C 2014 *Advanced Materials*
[5] Onal C D, Tolley M T, Rus D and Wood R J 2014 *Mechatronics, IEEE/ASME Transactions on* **to be published**
[6] Felton S, Tolley M, Demaine E, Rus D and Wood R 2014 *Science* **345** 644–646
[7] Yi Y W and Liu C 1999 *Journal of Microelectromechanical Systems* **8** 10–17
[8] Bassik N, Stern G M and Gracias D H 2009 *Applied physics letters* **95** 091901–091901
[9] Guan J, He H, Hansford D J and Lee L J 2005 *The Journal of Physical Chemistry B* **109** 23134–23137
[10] Niiyama R, Rus D and Kim S 2014 Pouch motors: Printable/inflatable soft actuators for robotics *Robotics and Automation (ICRA), 2014 IEEE International Conference on* (IEEE) pp 6332–6337
[11] Hawkes E, An B, Benbernou N M, Tanaka H, Kim S, Demaine E D, Rus D and Wood R J 2010 *Proceedings of the National Academy of Sciences* **107** 12441
[12] Liu Y, Boyles J K, Genzer J and Dickey M D 2012 *Soft Matter* **8** 1764–1769
[13] Keller S L 2004 *American Journal of Physics* **72** 599–604
[14] Felton S M, Tolley M T, Onal C D, Rus D and Wood R J 2013 Robot self-assembly by folding: A printed inchworm robot *Robotics and Automation (ICRA), 2013 IEEE International Conference on* (IEEE) pp 277–282
[15] Felton S M, Tolley M T, Shin B, Onal C D, Demaine E D, Rus D and Wood R 2013 *Soft Matter*

[16] Tolley M T, Felton S M, Miyashita S, Aukes D, Rus D and Wood R J 2014 *Smart Materials and Structures* **23** 094006

[17] Tolley M T, Felton S M, Miyashita S, Xu L, Shin B, Zhou M, Rus D and Wood R J 2013 Self-folding shape memory laminates for automated fabrication *Intelligent Robots and Systems (IROS), 2013 IEEE/RSJ International Conference on* (IEEE) pp 4931–4936

[18] Shin B, Felton S M, Tolley M T and Wood R J 2014 Self-assembling sensors for printable machines *Robotics and Automation (ICRA), 2014 IEEE International Conference on* (IEEE) pp 4417–4422

[19] Felton S M, Tolley M T and Wood R J 2014 Mechanically programmed self-folding at the millimeter scale *Automation Science and Engineering (CASE), 2014 IEEE International Conference on* (IEEE) pp 1232–1237

[20] Whitney J P, Sreetharan P S, Ma K Y and Wood R J 2011 *Journal of Micromechanics and Microengineering* **21** 115021

[21] Sreetharan P S, Whitney J P, Strauss M D and Wood R J 2012 *Journal of Micromechanics and Microengineering* **22** 055027

[22] Tachi T 2010 *Visualization and Computer Graphics, IEEE Transactions on* **16** 298–311

[23] Aukes D M, Goldberg B, Cutkosky M R and Wood R J 2014 *Smart Materials and Structures* **23** 094013